

## Auger photoelectron coincidence spectroscopy studies: Trends in the $L_{2,3}\text{-}M_{4,5}M_{4,5}$ line shapes across the 3d transition-metal series

C. P. Lund and S. M. Thurgate

*School of Physical Sciences, Engineering and Technology, Murdoch University, Murdoch WA 6150, Australia*

A. B. Wedding

*School of Applied Physics, University of South Australia, The Levels SA 5095, Australia*

(Received 11 July 1996)

The Auger-emission process from solids can be very complex, with a variety of processes producing intensity in the final spectra. The  $L_{2,3}\text{-}M_{4,5}M_{4,5}$  ( $L_{2,3}\text{-}MM$ ) Auger spectra of the 3d transition metals, in particular, show many complicating effects. Auger photoelectron coincidence spectroscopy (APECS) is a technique that can be used to elucidate the source of this complexity. In the APECS experiment, Auger electrons are recorded only when the corresponding electron from the ionization event is also detected. In this way only those features that result from the particular initial ionization event in question are measured, thereby greatly reducing the complexity in the Auger spectra. Although a number of successful APECS studies have been made of the emission processes observed in the Auger lines of several individual 3d transition metals, none have yet studied trends across the series. In order to study some of these trends we have made the most systematic APECS study to date of the  $L_{2,3}\text{-}MM$  Auger spectra of the metals Fe, Co, Ni, and Ga (in GaAs). The  $L_{2,3}\text{-}MM$  lines were observed in coincidence with the  $2p_{3/2}$  and  $2p_{1/2}$  photoemission electrons in all of these materials. From these studies and the Cu coincidence (APECS) results of Haak and Sawatzky a number of trends are clear and these are reported and discussed with the view of aiding quantitative Auger electron spectroscopy. It has become clear that there is also a need for a consistent and clear nomenclature to describe and distinguish between the various processes which can lead to a common multiple-hole final state. A nomenclature is proposed that aids a clearer comparison and discussion of the contributions of the various processes to the total observed Auger line shape. [S0163-1829(97)01107-7]

### INTRODUCTION

Auger spectroscopy is widely used as a technique for making quantitative estimates of the concentration of elements in surface studies. The Auger process is considerably more complex than the photoemission [x-ray photoemission spectroscopy (XPS)] process as it involves at least three electrons and the final state will have at least two additional holes in the electronic structure of the atom/solid. Indeed, in many elements/solids much of the complexity of Auger spectra is due to the interaction of the holes in the final state. Nonetheless, Auger spectra are often collected and processed with the view of finding concentrations of elements on surfaces as well as chemical or densities of states information.

In transition metals, the problems are particularly apparent. The high density of filled and unfilled states near the Fermi level increases the probability of shake off/shake up events accompanying the formation of both the initial state and the final state. These processes can have a dramatic effect on the Auger line shape. The high density of filled states also increases the chance of Coster-Kronig<sup>3</sup> (CK) events. The situation is also complicated by the fact that extrinsic processes are associated with the escape of the electron through the solid. These are often not easily accounted for. This makes it difficult to decide which parts of the Auger line shape can be attributed to intrinsic processes and which parts to extrinsic processes.

Auger photoelectron coincidence spectroscopy (APECS) provides an opportunity to simplify complex Auger spectra. The technique was successfully demonstrated by Haak and colleagues<sup>1,2</sup> and has been used successfully by two other groups since.<sup>4,5</sup> In an APECS experiment, Auger electrons are only recorded when the corresponding photoelectron is also recorded. Details of the technique and its applications have been recently reviewed by Thurgate.<sup>6</sup>

The 3d transition metals are among the most useful materials for engineering and manufacturing purposes. Consequently, they are materials that are often characterized in surface analysis systems and an understanding of those processes that influence their Auger line shapes is important and useful information. We have collected APECS data from a series of 3d transition metals over a period of several years with selections of these data published previously.<sup>7-11</sup> In this work we have brought these data and the Cu data of Sawatzky and Haak<sup>1,2</sup> together with an analysis of the trends in the data to present a systematic study of the elements of the 3d transition series from Fe to Ga (in GaAs).

The 3d transition metals contain nine elements ranging from the alkali-earth calcium to the noble-metal copper. In this range, the empty 3d shell is progressively filled in. The stable room-temperature forms of the transition elements are either monatomic fcc or bcc Bravais lattices, or hcp structures.<sup>12</sup> The d band lies high up in the conduction band, extending through the Fermi energy and this significantly influences the observed Auger lines. Three trends are evident

TABLE I. Trends in the physical and electronic properties of the 3*d* transition metals.

3 <i>d</i> transition metal	Structure (Ref. 13)	Valence bandwidth ( $\Gamma$ ) in eV (Ref. 14)	$\Delta E_{\text{core}}$ for $2p_{1/2}$ and $2p_{3/2}$ core levels in eV (Ref. 15)	Two 3 <i>d</i> hole interaction energy ( $U$ ) in eV (Ref. 14)
Fe	bcc	3.5	13.2	1.25
Co	hcp	3.25	15.05	1.25
Ni	fcc	3.0	17.4	2.5
Cu	fcc	2.75	19.8	8.0
Zn	hcp	1.75	23.1	9.6
Ga	complex	1.75	27.0	11.25

in the valence and core levels of the 3*d* transition metals when moving across the series. These are as follows: (i) a decreasing valence bandwidth ( $\Gamma$ ), (ii) that the Fermi energy ( $E_{\text{Fermi}}$ ) moves to the top of the band, and (iii) the energy separation of the  $2p_{1/2}$  and  $2p_{3/2}$  core levels ( $\Delta E_{\text{core}}$ ) increases. Each of these are known to effect the Auger line shapes of the 3*d* transition metals. The trends in a number of properties including the crystal structure, valence bandwidth, and  $2p_{1/2}/2p_{3/2}$  energy separation of the 3*d* transition metals are summarized in Table I.

### EXPERIMENT

The apparatus and techniques for collecting the APECS data have been described in detail previously.<sup>5,9</sup> The data were collected using a specially built APECS spectrometer based on a pair of 127° electron analyzers designed to have very good timing resolution. The samples were irradiated with Mg *K* $\alpha$  x-rays from a conventional, unmonochromated, x-ray source. The total time spread through the analyzers and their electronics was 1.6 ns and the analyzers were operated in a constant pass energy mode with a resolution of  $\approx 2.6$  eV. The rather poor resolution was a consequence of the high pass energy selected to give optimum count rates. As is characteristic of the present state of development of APECS systems, it took about 30 days to collect a spectrum with between approximately 600 and 1200 true coincidence counts at the main peak energy. The reasons why APECS spectra are so difficult to acquire have been fully discussed elsewhere.<sup>6</sup>

The samples included Fe and Co prepared from foil, and Ni as a single crystal. The GaAs sample was a high-purity commercially produced *p*-type single-crystal ingot, cleaved along the (110) plane. All samples were initially cleaned by *in situ* cycles of ion bombardment and short periods ( $\sim 3$  min) of heating to  $\sim 700$  °C (GaAs  $\sim 350$  °C) until the oxygen 1*s* photoelectron line was below detection by conventional XPS. After this the samples were repeatedly ion bombarded with 1-keV Ar<sup>+</sup> ions and heat treated ( $\sim 700$  °C) every 12 h. The GaAs samples were not heated above 350 °C and the Ga and As *M*-*VV* Auger line heights were consistent with a near to stoichiometric surface, although the surface may have been slightly Ga enriched. After 12 h of data collection no evidence of oxygen or carbon contamination was found on any of the samples except Fe. Despite the Fe sample being cleaned every 12 h a small amount of oxygen contamination was found on this surface

[see Fig. 1(b)] and was unavoidable due to the long counting times required to collect the data.

A strength of the APECS technique is that the one set of raw data produces both the coincidence data and the conventional XPS singles data free from any distortion due to instrumental changes. A more detailed description of the method for obtaining the coincidence spectra and the singles spectra from the accidental background in APECS has been described elsewhere.<sup>9</sup> The analyzer that was scanning either the photoelectron or Auger spectra was repeatedly swept through the energy range of interest a number of times during each 12 h data acquisition period in order to ensure that the spectra were free from any artifact due to contamination.

### DISCUSSION

The singles Auger spectra of the transition metals with *d* bands and the elements which follow them in the Periodic Table are shifted to lower kinetic energy than expected from the difference in the binding energies of the initial core hole and the self-convolution single-electron density of states. This indicates that the two-hole final states,  $\{d^2\}$ , formed in the Auger process are more tightly bound than the sum of the binding energies of the two single-hole states,  $\{d\} + \{d\}$ . As well as this the singles Auger lines of some of the elements show a number of sharp features<sup>16-19</sup> which have splittings in agreement with those of a  $\{d^2\}$  atomic configuration. Such spectra have been classified as quasiautomic<sup>16</sup> and the idea

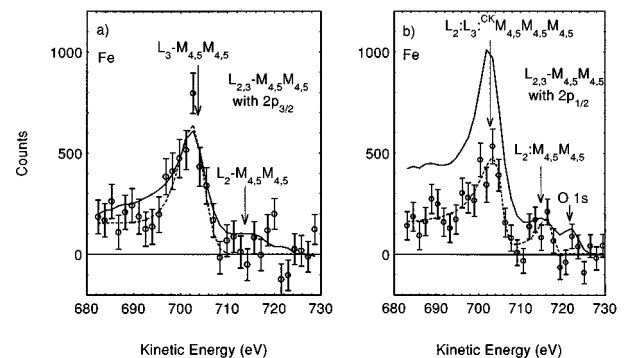


FIG. 1. The  $L_{2,3}\text{-}M_{4,5}M_{4,5}$  spectra of Fe in coincidence with (a) the  $2p_{3/2}$  photoelectron and (b) the  $2p_{1/2}$  photoelectron. The solid line is the singles spectrum which is also determined from the same set of raw data, while the dashed line is the best fit of a model spectrum to the data as explained in the text.

that they have atomic profiles has been confirmed by a number of authors.<sup>17-19</sup>

Cini<sup>20,21</sup> and Sawatzky<sup>22,23</sup> separately suggested that quasiatomic Auger spectra arise when the correlation energy between two holes localized on one atomic site,  $U$ , is much greater than the single-electron bandwidth,  $\Gamma$ , of the material. This ‘‘Cini-Sawatzky’’ model has been the basis for understanding correlation effects in Auger line shapes. According to the Cini-Sawatzky theory if the effective Coulomb repulsion is large compared to the bandwidth ( $U \gg \Gamma$ ), the line shape will be atomiclike, whereas if  $\Gamma \ll U$  the line shape will be bandlike. In systems where  $U \approx \Gamma$ , both atomiclike and bandlike contributions can be evident in the line shape.<sup>20-23</sup>

The analysis as presented by Cini and Sawatzky<sup>20-23</sup> was derived assuming an initially filled single band so that it is not rigorously valid for partially filled, or degenerate bands.<sup>14</sup> A more general intuitive explanation, that holds for filled and unfilled bands involves the position of the final-state energy levels relative to the band. If the final-state energy levels from which the Auger electron is ejected are pulled clear of the band following the initial ionization, this results in these elements exhibiting atomiclike peaks, if the final-state energy levels still lie in the band then the peaks will be bandlike. This behavior is reflected in the  $L_{2,3}$ - $MM$  Auger spectra of the  $3d$  transition metals.

The  $L_{2,3}$ - $MM$  spectrum in coincidence with the main  $2p_{3/2}$  ionization peak is free of contributions from processes such as

$$L_2-L_3M_{4,5}-M_{4,5}M_{4,5}(M_{4,5}),$$

which is an Auger cascade via a Coster-Kronig transition,  $L_2-L_3M_{4,5}$ . The bracketed  $M_{4,5}$  hole in the final state indicates that it is a spectator hole. A Coster-Kronig (CK) transition<sup>3</sup> is an Auger transition in which the principle quantum number of the initial hole and any of the two final holes is the same. In this case the process above with the  $2p_{3/2}$  electron filling the  $2p_{1/2}$  photoionization hole is a Coster-Kronig process as the two electrons are from orbitals with the same principle quantum number, in this case the  $2p$  orbitals. Coster-Kronig transition rates, which are large due to the large overlap of the radial wave functions of orbitals from the same shell, are very energy sensitive.<sup>16</sup> Furthermore, since the relative separation of different atomic levels varies with atomic number,  $Z$ , some CK transitions are only energetically possible for restricted ranges of atomic number. The large transition rates of CK processes cause them to dominate the cascade of Auger and radiative decays which follow the creation of inner-shell holes and thus they have a large effect on Auger and fluorescence yields.<sup>24,25</sup> They com-

pete directly with x-ray and Auger transitions and the doubly ionized states they produce give rise to satellites accompanying the x-ray and Auger spectra observed from singly ionized species.

Doubly ionized states which give rise to Auger vacancy satellites can be created by mechanisms other than Coster-Kronig transitions.<sup>26</sup> Two other such mechanisms are electron ‘‘shake off’’ and ‘‘shake up,’’ sometimes called monopole ionization and monopole excitation, respectively. As a result of a sudden change in the central potential of an atom, an electron in a given orbital may go into an excited (electron shake up) or continuum (electron shake off) state. The energy required for these transitions is not available to the main emission process and thus they lead to a structure on the low-kinetic-energy side of the spectral feature. Because the valence-band electron in a shake up transition is excited, but to a bound state, this will appear as a discrete satellite line at a kinetic energy lower than the peak energy of the main line. The energy difference corresponds to that between the ground and excited states of the ion with a core vacancy. In electron shake off, where the electron is excited into the continuum, the spectrum will show a continuous spectrum rising smoothly from a lower kinetic energy to a threshold whose energy difference is equal to the ionization potential for the ground state of the ion with a core vacancy.

The APECS  $L_3$ - $MM$  Auger line in coincidence with the  $2p_{3/2}$  photoelectron is also free from processes such as

$$L_3M_{4,5}-M_{4,5}M_{4,5}(M_{4,5}),$$

because the energy of the initial-state photoelectron is shifted due to the initial-state shake up/shake off of the  $M_{4,5}$  valence electron and hence is not detected. Whitfield and colleagues<sup>26</sup> have demonstrated using synchrotron measurements the presence of a number of initial-state processes that can lead to three or four holes in the final state and that can result in satellites in the  $L_3$ - $MM$  Auger spectra. They proposed that a three-hole final state could be produced via the following processes:

Process	Label/descriptor
(i) $L_1-L_3M_{4,5}-M_{4,5}M_{4,5}(M_{4,5})$	$L_1:L_3: {}^{\text{CK}}MMM$
(ii) $L_2-L_3M_{4,5}-M_{4,5}M_{4,5}(M_{4,5})$	$L_2:L_3: {}^{\text{CK}}MMM$
(iii) $L_3M_{4,5}-M_{4,5}M_{4,5}(M_{4,5})$	$L_3: {}^{\text{is}}MMM$

where (i) and (ii) are CK processes while (iii) is an initial-state shake up/shake off process. In addition to these, there are four ways a four-hole final state can be produced providing satellite intensity in the  $L_3$ - $MM$  spectrum. These are

Process	Label/descriptor
(iv) $L_1-L_2M_{4,5}-L_3M_{4,5}(M_{4,5})-M_{4,5}M_{4,5}(M_{4,5}M_{4,5})$	$L_1:L_2:L_3: {}^{\text{CK}}M^{\text{CK}}MMM$
(v) $L_1M_{4,5}-L_3M_{4,5}(M_{4,5})-M_{4,5}M_{4,5}(M_{4,5}M_{4,5})$	$L_1:L_3: {}^{\text{is}}M^{\text{CK}}MMM$
(vi) $L_2M_{4,5}-L_3M_{4,5}(M_{4,5})-M_{4,5}M_{4,5}(M_{4,5}M_{4,5})$	$L_2:L_3: {}^{\text{is}}M^{\text{CK}}MMM$
(vii) $L_3M_{4,5}M_{4,5}-M_{4,5}M_{4,5}(M_{4,5}M_{4,5})$	$L_3: {}^{\text{is}}(MM)MM$

There does not appear to be a consensus in the literature as to the best notation to identify/describe the various processes which generate particular hole states. This can be confusing and ambiguous, particularly in the description of processes that produce four or more holes in the final state. In an attempt to remove the confusion which can arise in describing the sequence of excited-state decay (hole state formation) and/or to have a nomenclature which makes clear the logical development of excited hole states and the emission resulting from the decay process, we propose the adoption of the following symbolism which is largely consistent with that of Whitfield.<sup>26</sup> We propose that all descriptions consist of the sequence of hole state formation (reading left to right) where the first hole represents the hole creation, either the initial photoionization or the level from which the hole in the previous state is filled, subsequent nonbracketed holes are those that contribute to electron emission. As mentioned earlier, brackets are used to indicate spectator holes. This allows the ready identification of such processes as final-state shake up/shake off, that is,  $M_{4,5}M_{4,5}M_{4,5}$  as distinct from emission in the presence of a hole  $M_{4,5}M_{4,5}(M_{4,5})$  as well as making the presence of one or more spectator holes immediately apparent. Superscripts preceding the hole level identifier could be used to label shake up/shake off and Coster-Kronig transitions when required. It has become apparent that the historical Auger line descriptor,  $ABC$  which describes a process not a hole state is not sufficiently descriptive and unambiguous and should be replaced with the hole state descriptor  $A-BC$ .

Process (iv) above is then easily identified as due to two consecutive CK processes resulting in a four-hole final state and culminating in the emission of a valence-band electron in the presence of two spectator holes. Process (v) has a shake up/shake off in the initial state ( $L_1M_{4,5}$ ) followed by a CK into the  $L_1$  hole to give the four-hole final state. Process (vi) is similar, but involves a CK into the  $L_2$  hole. Process (vii) involves a double shake up/shake off in the initial ionization to produce the intermediate three hole state,  $L_3M_{4,5}M_{4,5}$  which, with the emission of the Auger electron results in four holes in the final state.

In order to facilitate a repeated reference to each process within a given text and the clearer comparison and discussion of the contribution of the various processes to the total observed Auger and photoelectron spectra, we also propose the use of a shorthand label/descriptor for each process. This descriptor consists of a notation which indicates the initial photoionization hole and following a colon, the origin of each hole in the final-hole state in their order of generation. This allows the immediate identification of processes such as double initial state shakes as described in process (vii),  $L_3:is(MM)MM$  which would contribute intensity to the  $L_3:MM$  Auger line as a satellite which is shifted in energy from the main  $L_3-MM$  peak due to the interaction of the emitted Auger electron with the two spectator holes in the valence band. More importantly the origin of the two spectator holes is clearly identified as being created by an initial-state double shake process as distinct from a Coster-Kronig cascade  $L_1:L_2:L_3:CKMCKMMM$  as in process (iv) or an initial-state shake followed by a CK decay  $L_1:L_3:isMCKMMM$  as in process (v).

## Iron

Fe has the electron configuration  $[Ar]3d^64s^2$ . The valence bandwidth of Fe ( $\Gamma=3.5$  eV) is wide compared to the interaction energy of the final-state holes ( $U=1.25$  eV), therefore, the energy of the level from which the Auger electron is ejected lies in the valence band just prior to its ejection. This means Fe is seen to generate a bandlike Auger line and the line shape can be viewed as a weighted self-convolution of the densities of states.<sup>27</sup>

The  $L_{2,3}-M_{4,5}M_{4,5}$  Auger lines in coincidence with the  $2p_{3/2}$  and  $2p_{1/2}$  photoemission lines for Fe are shown in Figs. 1(a) and 1(b), respectively. Each of the coincidence spectra were fitted with a model spectrum which is the sum of one or more Gaussians and is shown as the dashed line. The least-squares fit was achieved using the Simplex algorithm,<sup>28</sup> as used in the fitting of XPS line shapes by Thurgate and Erickson.<sup>29</sup> A good fit was determined on the basis of a point by point least-squares comparison between the model curve and the coincidence data. A simple smoothly varying background function, to approximate the extrinsic loss function, has also been added to the sum of the component curves to give the total, fitted curve and adjusted to describe the intensity in the low-energy tail of the lines. The Fe  $L_3-MM$  spectrum in coincidence with the  $2p_{3/2}$  photoelectron is best described as a broad smoothly varying function with no indication of atomiclike features. This line shape contains only those features that arise from the  $2p_{3/2}$  ionization and is bandlike, reflecting the self-convolution of the valence-band densities of states.

The APECS Auger spectra obtained in coincidence with the  $2p_{3/2}$  photoelectron does not include initial-state processes that result in three or four holes in the final state such as those discussed above. This is because the photoelectron involved in these initial-state processes has an energy that is different from that of the photoelectron that is being detected in coincidence with the main two-hole Auger process and is outside the detection energy range of the photoelectron analyzer. Hence the  $2p_{3/2}$  coincidence spectra are free from many of the factors that complicate regular or conventional, singles Auger spectroscopy. The coincidence spectra in Fig. 1 do however include some processes that result in three holes in the final state such as

$$L_3-M_{4,5}M_{4,5}^{fs}M_{4,5}, \quad L_3:MM^{fs}M,$$

which represents a final-state shake up/shake off associated with the emission of the  $M_{4,5}$  Auger electron, as well as a range of possible final-state configurations with four or more holes. The coincidence experiment is not able to discriminate against these final-state processes as the ejected photoelectron has the same energy as that which initiates the main two-hole Auger  $L_3:MM$  process.

The Fe  $L_{2,3}-MM$  Auger spectrum collected in coincidence with the  $2p_{1/2}$  line [Fig. 1(b)] shows the main  $L_2:M_{4,5}M_{4,5}$  Auger component and the emission from the Coster-Kronig preceded Auger decay,  $L_2-L_3M_{4,5}-M_{4,5}M_{4,5}(M_{4,5})$ . This  $L_2:CKMMM$  component appears under the  $L_3-MM$  part of the singles  $L_{2,3}-MM$  line but is shifted to higher kinetic energy by 0.8 eV relative to the  $L_3:MM$  component. The line shape and energy position

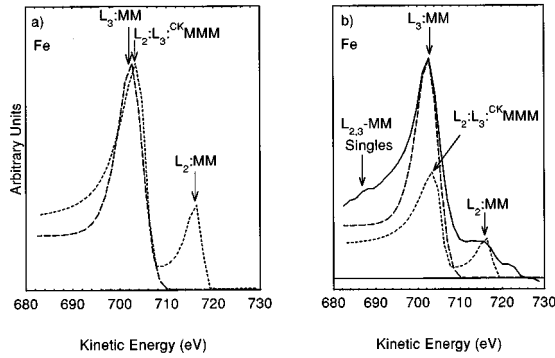


FIG. 2. Modeled Coster-Kronig shifted  $L_2:L_3:^{CK}M_{4,5}M_{4,5}M_{4,5}$  (short dash) and two-hole  $L_3:M_{4,5}M_{4,5}$  (long dash) contributions to the Fe  $L_3-MM$  coincidence data from Fig. 1 overlaid for comparison. (a) shows the two coincidence spectra normalized to the height of the  $L_3:MM$  part of the  $2p_{3/2}$  coincidence spectrum in order to more clearly compare the FWHM's. (b) shows the two spectra normalized to the singles spectrum (solid line) at the points indicated to enable an appreciation of the magnitude of the CK contribution to the line shape.

of this component can be taken as typical of those contributions due to all initial-state processes which generate a final three-hole state in Fe. Sawatzky<sup>2</sup> has shown from total-energy calculations that it is possible to estimate this energy difference between the three-hole final-state component and the main two-hole component. The energy shift of a  $L_3:isMMM$  or  $L_1:L_3:^{CK}MMM$  (three-hole) process compared to the  $L_3:M_{4,5}M_{4,5}$  (two-hole) process is given by<sup>2</sup>

$$\Delta E = \Delta E_{at} + \Delta R_{ea}. \quad (1)$$

The first term,  $\Delta E_{at}$ , is the atomic part of the Auger energy shift, the second term,  $\Delta R_{ea}$ , is the shift due to the difference in extra-atomic relaxation. The extra-atomic relaxation energy causes a reduction in Coulomb repulsion energy due to the interaction of a hole with the polarization cloud of the other holes present and hence a reduced kinetic energy for the emitted electron.

Figure 2 shows the CK shifted and normal Auger two-hole contributions to the Fe  $L_3-MM$  line together for comparison. (a) shows the two spectra normalized to the same height and the energy scale of the  $2p_{1/2}$  coincidence spectrum adjusted so that the main  $L_3-MM$  two-hole and CK shifted component peaks have the same energy, in order to compare their [full width at half maximum (FWHM)]. (b) shows the two coincidence spectra normalized to the height of the  $L_{2,3}-MM$  singles spectrum at the points shown, in order to compare their relative contributions. The two-hole component (coincident with the  $2p_{3/2}$  photoelectron) has been normalized so that its height matches the  $L_3MM$  part of the singles spectrum. Both the singles and coincidence spectra will have the intensity shifted from the region of the two-hole  $L_2-MM$  component to that of the CK shifted  $L_3-MM$  component in the same way. The CK shifted component (coincident with the  $2p_{1/2}$  photoelectron) has been normalized so that its height matches that of the two-hole  $L_2-MM$  part of the  $L_{2,3}-MM$  singles spectrum (at the point shown) because this region contains predominantly intensity only from the two-hole  $L_2-MM$  region of both spectra.

In Fe it is interesting to note that the line shape of the  $L_2:L_3:^{CK}MMM$  CK component is very similar to that generated by the  $L_3:MM$  two-hole final state, with both having the same FWHM within experimental error,  $6.3 \pm 0.1$  and  $6.5 \pm 0.1$  eV, respectively (Table II). It seems that the additional electrostatic interaction generated by the presence of the spectator hole does not shift the levels in the final state clear of the valence band in Fe. This means the line shape due to the Coster-Kronig preceded  $L_2:L_3:^{CK}MMM$  three-hole final-state process remains bandlike.

### Cobalt

The  $L_{2,3}-M_{4,5}M_{4,5}$  Auger spectra in coincidence with the  $2p_{3/2}$  and  $2p_{1/2}$  photoelectrons for Co are shown in Fig. 3. Like Fe, the  $L_3:MM$  two-hole final state produces a bandlike Auger line, as can be seen from the broad  $L_3:MM$  component in coincidence with the  $2p_{3/2}$  photoelectron [Fig. 3(a)]. Figure 4 shows the CK shifted and the normal Auger two-hole contributions to the Co  $L_{2,3}-MM$  spectra together

TABLE II. Contribution of the Coster-Kronig  $L_2:L_3:^{CK}M_{4,5}M_{4,5}M_{4,5}$  transition to the  $L_3-M_{4,5}M_{4,5}$  Auger line across the 3d transition series.

3d transition metal	Energy shift $\Delta E$ in the $L_2:L_3:^{CK}MMM$ Coster-Kronig component relative to the $L_3:MM$ two-hole component in eV	Ratio of the peak area of the $L_3:MM$ component to the $L_2:L_3:^{CK}MMM$ Coster-Kronig component	FWHM of the two-hole $L_3:MM$ component	FWHM of the $L_2:L_3:^{CK}MMM$ Coster-Kronig component	Ratio of the FWHM of the $L_3:MM$ to $L_2:L_3:^{CK}MMM$ components
Fe	$+0.8 \pm 0.2$	$4.3 \pm 0.6$	$6.5 \pm 2\%$	$6.3 \pm 2\%$	$1.03 \pm 0.01$
Co	$-1.1 \pm 0.2$	$13:1 \pm 2$	$5.9 \pm 2\%$	$3.7 \pm 2\%$	$1.62 \pm 0.06$
Ni	$-0.0 \pm 0.2$	$5.1:1 \pm 0.8$	$7.4 \pm 2\%$	$2.5 \pm 2\%$	$3.0 \pm 0.1$
Cu <sup>a</sup>	$-5.5 \pm 0.5$	$1.9:1 \pm 0.2$	$6.0 \pm 2\%$	$4.6 \pm 2\%$	$0.59 \pm 0.06$
Ga	none	No CK	No CK	No CK	No CK

<sup>a</sup>The Cu values are taken or calculated from the results of Sawatzky (Ref. 2).

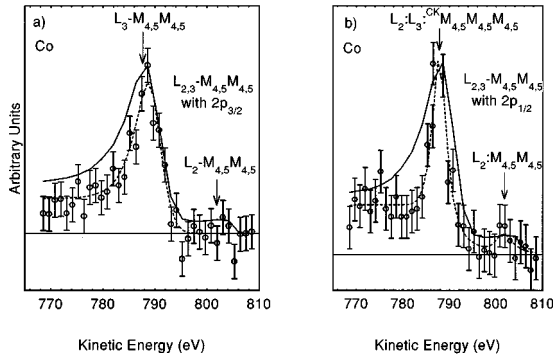


FIG. 3. The  $L_{2,3}\text{-}M_{4,5}M_{4,5}$  spectra of Co in coincidence with the (a)  $2p_{3/2}$  photoelectron and (b)  $2p_{1/2}$  photoelectron. The solid line is the singles spectrum while the dashed line is the best fit of a model spectrum to the data.

for comparison in the same way as for Fe. This shows that unlike Fe, the Auger line of Co is noticeably modified by the presence of an additional hole. The centroid of the  $L_2:L_3:\text{CKMMM}$  CK shifted peak in coincidence with the  $2p_{1/2}$  peak has moved 1.1 eV to lower-kinetic-energy relative to the two-hole  $L_3:MM$  component and has narrowed from a FWHM of  $5.9 \pm 0.1$  eV for the two-hole component to a FWHM of  $3.7 \pm 0.1$  eV. This is a clear indication of an increase in the hole-hole interaction energy due to the extra hole in the final state, causing a modification of the line shape as predicted by the Cini-Sawatzky<sup>20-23</sup> theory. Of course this has the added implication that the singles Auger line is highly modified by the presence of the CK preceded  $L_2:L_3:\text{CKMMM}$  process.

### Nickel

The  $L_{2,3}\text{-}M_{4,5}M_{4,5}$  Auger spectra of Ni are complex. Ni is towards the end of the  $3d$  transition series, and starts to illustrate some limiting behavior. It has been recognized for some time<sup>30</sup> that the  $L_{2,3}\text{-}M_{4,5}M_{4,5}$  Auger line of Ni has both a quasiautomatic component and a bandlike component. The

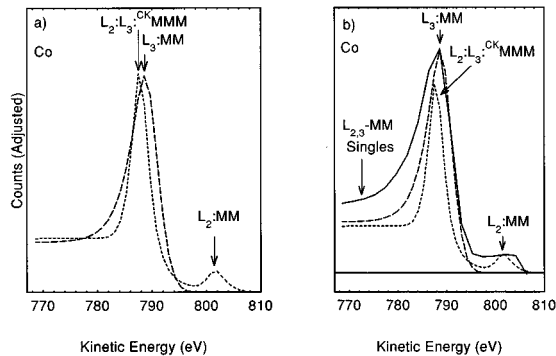


FIG. 4. Modeled  $L_2:L_3:\text{CKMMM}$  Coster-Kronig shifted (short dash) and  $L_3:M_{4,5}M_{4,5}$  two-hole (long dash) contributions to the Co  $L_3\text{-}M_{4,5}M_{4,5}$  coincidence data from Fig. 3 overlaid for comparison. (a) shows the two coincidence spectra normalized to the height of the  $L_3:M_{4,5}M_{4,5}$  part of the  $2p_{3/2}$  coincidence spectrum in order to more clearly compare the FWHM's. (b) shows the two coincidence spectra normalized to the singles spectrum (solid line) at the energies indicated, which reflects their respective ratios.

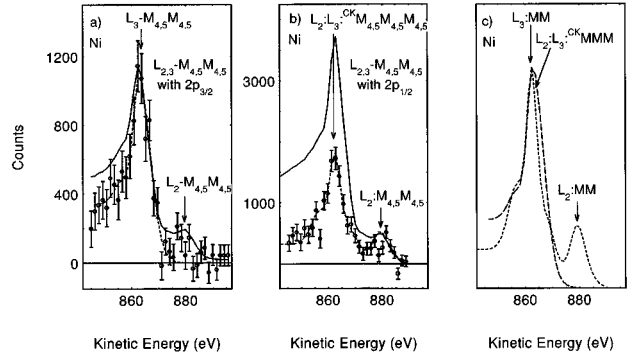


FIG. 5. The  $L_{2,3}\text{-}M_{4,5}M_{4,5}$  spectra of Ni in coincidence with (a) the  $2p_{3/2}$  photoelectron and (b) the  $2p_{1/2}$  photoelectron showing the singles (solid line) scaled at the points indicated and overlaid with the raw data for comparison and a model fit to the coincidence data (short dash). (c) shows the model Coster-Kronig shifted  $L_2:L_3:\text{CKMMM}$  coincidence spectrum and the main two-hole  $L_3:M_{4,5}M_{4,5}$  (long-dash) coincidence contribution to the Ni  $L_{2,3}\text{-}M_{4,5}M_{4,5}$  line overlaid and normalized to the same peak height for comparison of their FWHM's.

quasiautomatic part is due to those final-state configurations where the levels are pulled out of the valence band. Ni has a ground-state electron configuration of  $[\text{Ar}]3d^84s^2$ . As can be seen in Table I, the valence bandwidth of Ni ( $\Gamma = 2.5$  eV) is narrower than that of Co or Fe while the two  $3d$  hole interaction energy ( $U = 3.0$  eV) is larger. Ni has a  $U/\Gamma$  ratio of 1.2 and this explains the complexity of the spectrum and the presence of the quasiautomatic component.

The Ni  $L_{2,3}\text{-}M_{4,5}M_{4,5}$  spectra in coincidence with the  $2p_{3/2}$  and  $2p_{1/2}$  photoelectrons are shown in Fig. 5. The spectra have been fitted by up to three-component peaks using the simplex fitting program described above, and a model based on the work of Haak<sup>1</sup> and Sawatzky<sup>2</sup> and Mårtensson and colleagues.<sup>30</sup> Figure 5(c) shows both the model spectra normalized to the height of the  $2p_{3/2}$  coincidence spectrum and the  $2p_{1/2}$  coincidence spectrum energy shifted to overlay the main peaks for a better comparison of the FWHM's. The various atomic and bandlike contributions used in the model to fit the original spectra are shown in Figs. 6(a) and 6(b). The sum of the components of the model Ni  $2p_{3/2}$  and  $2p_{1/2}$  coincidence spectra are shown normalized to the same height, that of the main peak in the  $2p_{3/2}$  model spectrum, and overlaid for comparison in Fig. 6(c). The three peaks in the  $2p_{3/2}$  spectrum correspond to the main atomiclike terms, a component due to a  $3d^7$  final state and the bandlike component. The  $3d^7$  final-state component lies at the lowest kinetic energy and comes from an initial  $3d^9$  configuration as discussed by Sawatzky.<sup>2</sup> The atomiclike peak is the normal two-hole peak and contains the sum of peaks that come from the decay into the  $3d^8$  final state. Individual atomic component peaks are too close to be resolved by the resolution of our analyzer ( $\sim 2.6$  eV). The bandlike component is at the highest kinetic energy.

It is interesting to note the differences between the Co [Fig. 3(b)] and Ni [Fig. 5(b)]  $2p_{1/2}$  coincidence lines. The Co line is bandlike and narrowed by the increased hole-hole interaction. If there was an atomiclike contribution intensity in Co it would be expected at the low-kinetic-energy side of the peak as the lines are pulled clear of the band, however this is

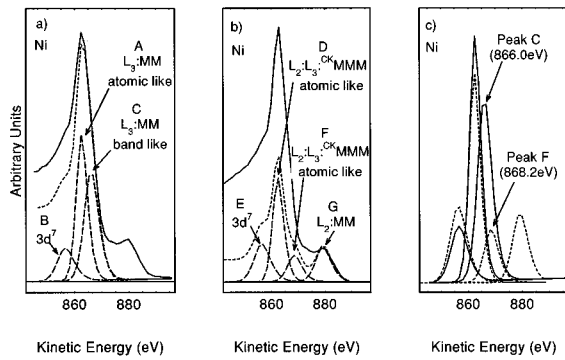


FIG. 6. The  $L_{2,3}M_{4,5}M_{4,5}$  spectrum of Ni in coincidence with (a) the  $2p_{3/2}$  photoelectron and (b) the  $2p_{1/2}$  photoelectron showing the singles (solid line), model fit to the coincidence data (short dash) and the model component peaks (long dash). The peaks A and B are the main atomiclike and  $3d^7$  components, respectively, and peak C is a bandlike contribution to the  $L_3$ -MM spectrum as explained in the text. The smoothly varying background function is not shown. Peaks D and E are the main atomiclike and  $3d^7$  components, respectively, of the  $2p_{1/2}$  coincidence spectrum. Peak F (which is at a higher kinetic energy than peak C) is unlikely to be the bandlike component but is most likely an atomiclike term from the doubly ionized Ni state as explained in the text. Peak G is the  $L_2$  component of the  $2p_{1/2}$  coincidence spectrum. (c) represents the overlay of the component peaks normalized to a common peak height for the total model spectra which clearly indicates the change in intensity of the bandlike component from the  $2p_{3/2}$  (solid lines) to the  $2p_{1/2}$  (dashed lines) spectrum.

not seen in Fig. 3. On the other hand, the Ni is predominantly atomiclike, as seen by the relative contributions required to describe the coincidence spectra in Fig. 6(b). The FWHM of the main atomiclike component (peak D) of the  $L_2$ -MM spectrum in coincidence with the  $2p_{1/2}$  photoelectron is  $6.0 \pm 0.1$  eV compared with a FWHM of  $7.4 \pm 0.1$  eV for the component in coincidence with the  $2p_{3/2}$  photoelectron (peak A). The main contribution to the  $L_2:L_3$ : $^{CK}MMM$  CK shifted component does not however appear to be shifted in energy relative to the main two-hole component (peak A), as was the case for Co.

Haak and Sawatzky<sup>1,2</sup> have measured the Ni  $L_3$ -MM Auger line in coincidence with the shake up/shake off satellite of the Ni  $2p_{3/2}$  photoelectron line. This was done by fixing one analyzer at 6 eV below the main  $2p_{3/2}$  photoelectron line at 858.2 eV and scanning the other analyzer over the Ni  $L_{2,3}$ -MM Auger line. The resulting coincidence Auger spectrum also showed intensity under the  $L_3$ -MM line that coincided within 0.2 eV with the energy of the maximum intensity of the normal  $L_3$ :MM two-hole component of the  $L_3$ -MM line. As Eq. (1) is independent of how the intermediate  $-L_3M_{4,5}$  state was produced, the intensity due to process (iii) would be expected to appear at the same energy as that due to process (ii). The data in Fig. 5(b) for the Ni  $L_{2,3}$ -MM Auger spectrum of pure Ni, taken in coincidence with the Ni  $2p_{1/2}$  photoelectron, show this to be the case, with the  $L_2:L_3$ : $^{CK}MMM$  CK component also appearing at the same energy (within 0.2 eV) as the  $L_3$ :MM two-hole component.

From Fig. 6(c) it can be seen that the bandlike component is present in the curve in coincidence with the  $2p_{3/2}$ , where

its area is  $71 \pm 5$  % of the main atomiclike contribution (peak B). From a careful analysis of the curve that is in coincidence with the  $2p_{1/2}$  photoelectron however it appears that the bandlike component is either significantly reduced or not present at all. This explains the apparent FWHM narrowing seen in the  $L_2:L_3$ : $^{CK}MMM$  CK shifted component in Fig. 5(c). It can be seen from Fig. 5(c) that the  $L_2:L_3$ : $^{CK}MMM$  CK shifted component does have a peak (peak F) on the high-kinetic-energy side of the atomiclike peak (peak D). This peak is however at a higher ( $\sim 2$ -eV) kinetic energy than the bandlike peak (peak C) in the  $2p_{3/2}$  spectrum. A good fit to the raw coincidence data could not be achieved for the  $2p_{1/2}$  spectrum with a peak at the energy of the bandlike component in the  $2p_{3/2}$  spectrum.

It is difficult to argue that this peak (peak F) is the bandlike component in Ni as the Cini-Sawatzky theory<sup>21-23</sup> predicts that due to a higher hole-hole interaction energy in the presence of the additional hole from the CK process the bandlike component would be narrowed and shifted to a lower kinetic energy, not higher. This was, for example, what was observed in Co (above) where the bandlike two-hole line shape (coincident with the  $2p_{3/2}$  photoelectron) was narrowed and shifted to a lower kinetic energy in the CK shifted component (coincident with the  $2p_{1/2}$  photoelectron). The peak on the high-kinetic-energy side of the  $L_2:L_3$ : $^{CK}MMM$  CK shifted component is unlikely to be due to the bandlike component but rather is more likely to be due to a new atomiclike term resulting from the decay of the doubly ionized  $1s^2 2s^2 2p^5 3d^8 4s^2$  ion rather than the singly ionized ion. Haak and Sawatzky<sup>1,2</sup> have shown that the effect of the additional hole on the atomiclike spectrum of Cu is to change the nature and position of the atomic terms. This is a consequence of the terms becoming those of the doubly ionized atom in the  $L_2:L_3$ : $^{CK}MMM$  CK shifted component rather than the singly ionized species.

## Copper

Haak and Sawatzky<sup>1,2,31</sup> have previously published high-resolution APECS spectra of copper and these are shown reproduced in Figs. 7(a) and 7(b) along with the corresponding singles spectra. Figure 7(a) shows the Cu  $L_{2,3}M_{4,5}M_{4,5}$  Auger spectrum in coincidence with the  $L_3$  ( $2p_{3/2}$ ) photoelectron line, while Fig. 7(b) is the same spectrum in coincidence with the  $L_2$  ( $2p_{1/2}$ ) photoelectron line. Cu has a bandwidth,  $\Gamma$ , of 8.0 eV and a two-hole interaction energy,  $U$ , of 2.75 eV ( $U/\Gamma = 2.9$ ). Therefore as expected from the Cini-Sawatzky theory<sup>20-23</sup> the two-hole final state produces a predominantly atomiclike spectrum. The solid line shown in the two coincidence curves is a computer generated fit by Haak and Sawatzky<sup>1,2</sup> based on the multiplet structure calculated by McGuire,<sup>32</sup> and using Lorentzians with a FWHM of 1.6 eV. A high-energy satellite "band" was fitted by Haak and Sawatzky<sup>1,2</sup> with a Gaussian (FWHM 5.5 eV). Each of the multiplet components and the band satellite are labeled in Fig. 7 for the coincidence spectra based on the work of Haak and Sawatzky.<sup>1,2</sup>

The band part of the  $2p_{3/2}$  coincidence spectrum on the high-kinetic-energy side of the  $^3F$  term was also predicted by the Cini-Sawatzky theory. The band intensity as measured by Haak and Sawatzky<sup>1,2</sup> from the coincidence spectrum is

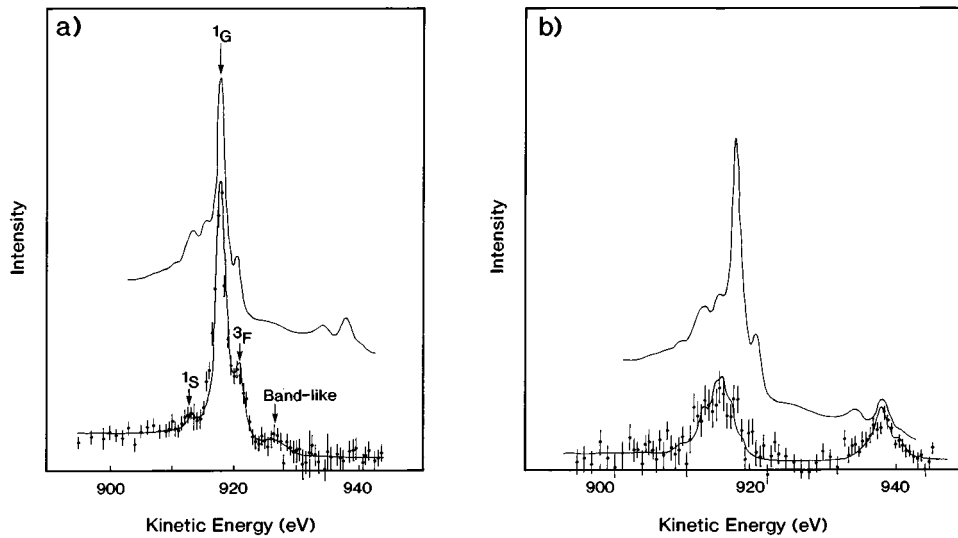


FIG. 7. The  $L_{2,3}\text{-}M_{4,5}M_{4,5}$  spectra of Cu in coincidence with (a) the  $2p_{3/2}$  photoelectron and (b) the  $2p_{1/2}$  photoelectron reproduced from those of Sawatzky and Haak (Refs. 1, 2, and 31). The singles spectra (solid line), the best fit by Sawatzky and Haak (Refs. 1, 2, and 31) of model spectra to the data (dashed line) and the atomic terms and bandlike contribution of Sawatzky (Ref. 2) are shown.

approximately 7% of the total. This value is close to the value of 5% calculated theoretically by Sawatzky<sup>2</sup> using the values obtained by Cini's<sup>33,34</sup> approximation and the theoretical intensities of the multiplet terms given by McGuire.<sup>32</sup> Figure 7(b) shows that the presence of the additional hole results in a  $\Delta E$  shift of 5.5–6.0 eV for the  $L_2:L_3:\text{CK}MMM$  CK shifted component relative to the main  $L_3:MM$  two-hole component, which is in good agreement with the semiempirical result of  $\Delta E=5$  eV calculated by Sawatzky<sup>2</sup> using Eq. (1). The effect of the additional hole on the spectrum of Cu is to change the nature and position of the atomic terms. This is a consequence of the terms becoming those of the doubly ionized atom in the  $L_2:L_3:\text{CK}MMM$  CK shifted component rather than the singly ionized species and results in the FWHM going from  $2.7\pm 0.1$  eV in the  $2p_{3/2}$  spectrum to  $4.6\pm 0.2$  eV in the  $L_2:L_3:\text{CK}MMM$  CK shifted component of the  $2p_{1/2}$  coincidence spectrum.

### Gallium (in GaAs)

Ga having a  $[\text{Ar}]3d^{10}4s^24p^1$  electron configuration is classed as being outside the  $3d$  transition metals. For Ga the final-state hole-hole interaction energy ( $U=11.25$  eV) is much greater than the valence bandwidth ( $\Gamma=1.75$  eV), that is  $U/\Gamma\gg 1$ , and the singles  $L_{2,3}\text{-}M_{4,5}M_{4,5}$  spectrum has been shown to be entirely atomiclike.<sup>35</sup> Antonides and colleagues<sup>36</sup> have also shown that there is very little probability of CK processes occurring in Ga and from high-resolution singles spectra there appears to be no evidence of three- or four-hole states.<sup>35,36</sup> Antonides and colleagues<sup>35</sup> have fitted the Ga  $L_{2,3}\text{-}M_{4,5}M_{4,5}$  spectra with the five final-state terms  $^1S$ ,  $^1G$ ,  $^3P$ ,  $^1D$ , and  $^3F$  and the  $L_3\text{-}M_{4,5}M_{4,5}$  line shape is well described by the atomic terms. Little is known of the shake up/shake off processes in Ga but the analysis of Antonides and colleagues<sup>35,36</sup> appears to show that they do not appear to be important in the  $L_{2,3}\text{-}M_{4,5}M_{4,5}$  Auger spectrum.

The Ga  $L_{2,3}\text{-}M_{4,5}M_{4,5}$  Auger line in coincidence with the  $2p_{3/2}$  and  $2p_{1/2}$  photoelectrons for GaAs are shown in Figs. 8(a) and 8(b), respectively. It can be seen that unlike the case

of the  $3d$  elements Fe-Cu the singles and coincidence spectra show good agreement in the region of the main  $L_2:MM$  and  $L_3:MM$  components of the  $L_{2,3}\text{-}MM$  Auger lines. This confirms the work of Antonides, Janse, and Sawatzky<sup>35</sup> that there are no significant CK or shake up/shake off processes operating in Ga. The main part of the  $L_2\text{-}MM$  and  $L_3\text{-}MM$  Auger lines can be well described using the atomic terms of a singly ionized atom. It can be seen in Fig. 8, however, that there are substantial differences between the singles and coincidence spectra in the region of the satellite between 11 and 16.5 eV below the main peaks. EELS (Refs. 37–39) and XPS (Ref. 40) spectra show that GaAs has a bulk-plasmon loss at 16.3 eV below the main line. Depending on the energy of the initial primary electrons and the particular surface (i.e., crystal face and which reconstruction is present), the surface plasmon has been known to vary from 10.0 to 11.5 eV below the main line.<sup>37–39</sup> Ludeke and Koma<sup>39</sup> have shown that at 400-eV primary energy on a GaAs (111) face

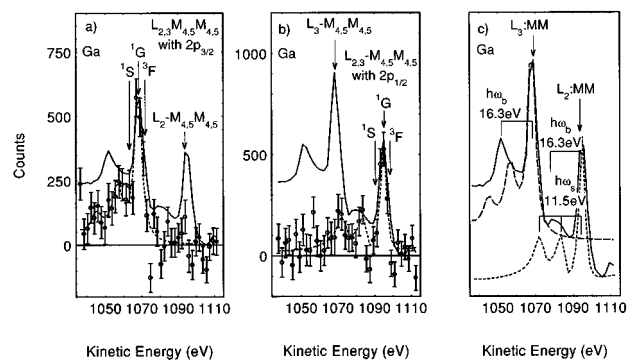


FIG. 8.  $L_{2,3}\text{-}M_{4,5}M_{4,5}$  Auger spectrum of Ga (in GaAs) in coincidence with (a) the  $2p_{3/2}$  and (b) the  $2p_{1/2}$  photoelectron lines. The coincidence spectra have been fitted with a model spectrum where the energy positions of each of the atomic term contributions to the main Ga DOS as given by Antonides and colleagues (Ref. 35) are marked. For comparison the model spectra are shown in part (c) as short-dashed ( $2p_{1/2}$ ) and long-dashed ( $2p_{3/2}$ ) curves while the regular singles spectrum is shown as a solid line. The bulk ( $h\omega_b$ ) and surface ( $h\omega_s$ ) plasmon energies for GaAs are shown.

there is a surface-plasmon loss at the energy of 11.5 eV as predicted by theory ( $\omega_S = \omega_b / \sqrt{2}$ ).

Figure 8(c) shows the singles spectra for the Ga  $L_{2,3}-M_{4,5}M_{4,5}$  Auger spectrum from GaAs together with both the  $L_{2,3}-M_{4,5}M_{4,5}$  in coincidence with the  $2p_{3/2}$  photoelectron lines and the  $L_{2,3}-M_{4,5}M_{4,5}$  in coincidence with the  $2p_{1/2}$  photoelectron overlaid for comparison. Each of the coincidence spectra have been fitted with a model spectrum using the Simplex program as above. The main, atomiclike component of each line (e.g., 1068 eV for  $L_3-M_{4,5}M_{4,5}$ ) was fitted with a single Gaussian as the analyzer resolution ( $\approx 2.6$  eV) did not allow differentiation between the various atomic term components. The positions of the atomic terms in the Ga DOS, as given in the work of Antonides and colleagues,<sup>35</sup> are however marked in Figs. 8(a) and 8(b). A good fit between the model and the experimental coincidence data was only achieved by fitting two Gaussians at multiples of 11.5 eV (the surface-plasmon energy) below the main peak and these values for the energy positions were fixed throughout the analysis. The peak intensities and full width at half maximum (FWHM) were then optimized using the Simplex algorithm.

Based on our coincidence results for GaAs, the work of Antonides and colleagues<sup>35</sup> for the Ga Auger line and the EELS spectra of GaAs,<sup>37-39</sup> we assign the low-energy satellite at  $\approx 16$  eV below the main peak in both our Ga  $L_2-M_{4,5}M_{4,5}$  and  $L_3-M_{4,5}M_{4,5}$  singles lines to a combination of the surface and bulk plasmons and not due to any intrinsic process. Differences between the singles and coincidence spectra for the  $L_{2,3}-M_{4,5}M_{4,5}$  spectrum in coincidence with the  $2p_{3/2}$  and  $2p_{1/2}$  photoelectron lines can be explained solely by the differences in inelastic mean free path (IMFP) for electrons of different energy. The singles spectrum is at an energy of  $\sim 1100$  eV, which corresponds to an IMFP (Ref. 41) of 23.7 Å, therefore it will show a combination of largely bulk-plasmon loss features with some contribution from surface-plasmon loss features.

The effective coincidence IMFP  $\lambda_{\text{eff}}$  is given by<sup>11</sup>

$$\frac{1}{\lambda_{\text{eff}}} = \frac{1}{\lambda_A} + \frac{1}{\lambda_{\text{PE}}}, \quad (2)$$

where  $\lambda_A$  is the IMFP of the Auger electron and  $\lambda_{\text{PE}}$  is the IMFP of the photoelectron. From this it can be seen that the electrons contributing to the coincidence line will have an IMFP of less than that of the photoelectron line (4.06 Å) (Ref. 41) and therefore come from much closer to the surface than those in the singles Auger line. The coincidence Auger line is therefore likely to be described predominantly by a surface loss function. In this case the surface-plasmon contribution can be expected to remain constant, while that of the bulk plasmon will be expected to decrease or disappear from the spectrum entirely. Figure 8 shows exactly the result expected in light of the previous discussion. The singles Auger spectra have a large satellite at  $\sim 16.3$  eV corresponding to the bulk plasmon, with a small shoulder at  $\sim 11.5$  eV corresponding to the surface plasmon. On the other hand, the coincidence spectra have only multiples of peaks separated by 11.5 eV corresponding to the surface plasmon with only a small intensity, if any, at 16.3 eV corresponding to the bulk plasmon. This difference in IMFP distance, 19.6 Å, for two

energies differing by  $\sim 1000$  eV is useful for showing the bulk and surface effects more clearly than conventional photoemission experiments. APECS has the advantage that this is achieved for the same surface from the same set of data at one time.

Similar results for the wide band, nearly free-electron metal Al have been reported by Jensen and colleagues.<sup>42</sup> Yubero and colleagues<sup>43</sup> have recently applied a proposed model for quantitative analysis of reflection electron-energy-loss spectra to evaluate the dielectric loss function of Si and SiO<sub>2</sub> in the 4–100-eV energy range, and to determine inelastic-scattering properties for these materials for low-energy electrons (500–10 000 eV). Their calculations of the effective inelastic-scattering cross sections as a function of the path traveled by the electron for different primary energies show clearly how the surface effects are enhanced at low primary electron energies. Slow electrons (e.g., 500 eV) reach depths of a few nanometers, and correspondingly excite more efficiently the surface plasmons rather than the bulk plasmons. More energetic electrons excite a larger number of bulk plasmons.

Although confirming the absence of complications due to intrinsic processes the coincidence results for Ga in GaAs show that care must still be taken when using the Ga  $L_{2,3}-M_{4,5}M_{4,5}$  Auger lines for quantitative analysis. Extrinsic loss processes and, in particular, second-order bulk and surface plasmons from the  $L_2-M_{4,5}M_{4,5}$  line can be seen to make a significant contribution to the  $L_3-MM$  line that must be correctly accounted for when using it for quantitative analysis. The same can also be argued to be true for the effect of the  $2p_{3/2}$  photoelectron line on the  $2p_{1/2}$  line. From Fig. 8 it can be seen that the second-order surface-plasmon loss peak from the  $L_2-MM$  line still has significant intensity and appears on the high-kinetic-energy side (1068–1072 eV) of the  $L_3-MM$  peak. This is one reason why the main component of the  $L_3-MM$  peak in coincidence with the  $2p_{3/2}$  is less intense than the singles peak on the high-kinetic-energy side as the two curves were normalized at the peak of the main component. From the results of Fig. 8 the second-order surface plasmon is of the order of  $15 \pm 5\%$  of the  $L_3-M_{4,5}M_{4,5}$  peak and will therefore significantly effect the quantitative results obtained using this peak if not correctly accounted for by an appropriate and correct background subtraction.

#### Trends in the Coster-Kronig rate and line shape of the Coster-Kronig preceded $L_2:L_3$ :<sup>CK</sup>MMM contribution across the 3d series

Except for very heavy elements, there have been few direct measurements of CK spectra<sup>44-46</sup> since they usually occur in the low-energy region of the electron spectrum, which is dominated by inelastically scattered electrons. Consequently, it is difficult using conventional Auger spectra to measure CK energies accurately and this lack of precision in energies creates very large uncertainties in calculated transition rates. For the  $L$  shell this difficulty has been mitigated by Chen and colleagues<sup>47</sup> who give an extensive compilation of free-atom Coster-Kronig energies derived from Dirac-Fock-Slater  $\Delta$ SCF calculations.

It is possible, in principle, to derive the overall Coster-Kronig rates from the coincidence data for the elements Fe to Cu presented above, though we would need at least one further measurement for each to compute the total ratio. This can be seen from the following analysis. If a  $2p_{1/2}$  hole is created, then the atom can relax by the following Auger processes:

1.  $L_2-M_{4,5}M_{4,5}$ ,
2.  $L_2-M_{2,3}M_{4,5}$ ,
3.  $L_2-M_{2,3}M_{2,3}$ ,
4.  $L_2-M_1M_{4,5}$ ,
5.  $L_2-M_1M_{2,3}$ ,
6.  $L_2-M_1M_1$ ,
7.  $L_2-L_3M_{4,5}-M_{4,5}M_{4,5}(M_{4,5})$ ,  
 $L_2:L_3:CKM_{4,5}M_{4,5}M_{4,5}$ ,
8.  $L_2-L_3M_{4,5}-M_{2,3}M_{4,5}(M_{4,5})$ ,  $L_2:L_3:CKM_{2,3}M_{4,5}M_{4,5}$ .

Given that the multiplicity of the  $3s$  processes involving the  $M_1$  level are not very significant. The  $L_2$  hole can also decay via x-ray emission in processes similar to those of 1–6 but the probability for these x-ray emission processes is substantially less than that for Auger decay.

Regular singles data can be used to find the sum of processes 2–6 relative to process 1. APECS spectra of the  $L_3-M_{4,5}M_{4,5}$  and  $L_3-M_{2,3}M_{4,5}$  Auger lines in coincidence with the  $2p_{1/2}$  can be used to find the sum of processes 7 and 8 relative to process 1. In this way a reasonable estimate of the probability of the Coster-Kronig preceded  $L_2-L_3M_{4,5}-M_{4,5}M_{4,5}(M_{4,5})$  process could be made. We have not yet gathered the data to enable a good estimate of the total CK processes for the  $3d$  transition metals.

We can however estimate how much of the  $L_3-M_{4,5}M_{4,5}$  Auger line is due to an  $L_2-L_3M_{4,5}-M_{4,5}M_{4,5}(M_{4,5})$  process. This is important as the Coster-Kronig contribution is subject to changes in the work function due to differing amounts of a single element in different alloy materials<sup>48</sup> as well as between different pure elements. The low binding energies of the  $3d$  orbitals coupled with large extra-atomic contributions to the Auger energy makes  $L_2:L_3:CKM_{4,5}M_{4,5}M_{4,5}$  CK transitions energetically possible for  $Z \leq 30$  (Ref. 16) though  $\Delta$ SCF calculations indicate that transitions are not allowed for free atoms.<sup>47</sup> This condition is easily satisfied for Cu ( $Z=29$ ), while for Zn ( $Z=30$ ) the  $M_{4,5}$  binding energy is close to the threshold for this process.<sup>49,50</sup> It is apparent in the singles Auger spectra of the  $3d$  transition metals that the  $L_2:MM$  component of the  $L_{2,3}-MM$  spectrum increases in intensity relative to the  $L_3:MM$  component with an increasing atomic number. Previous APECS studies of pure Ni and Ni/Fe alloys<sup>48</sup> have shown that the process of alloying can even change the rate of the  $L_2:CKM_{4,5}M_{4,5}M_{4,5}$  CK process for a single element when it is present in a number of different materials. The measured energy shift  $\Delta E$  and the amount of contribution of the  $L_2:L_3:CKM_{4,5}M_{4,5}M_{4,5}$  process to the  $L_3-MM$  Auger line relative to the main  $L_3$  two-hole process for the elements Fe to Cu as calculated from the coincidence data are shown in Table II.

## CONCLUSIONS

This is the most comprehensive Auger photoelectron coincidence spectroscopy (APECS) study to date of the

$L_{2,3}-MM$  Auger line shapes of the  $3d$  transition metals, across the row of the Periodic Table, from the bandlike Fe to the atomiclike Ga. These have enabled a study of a number of important trends across this series. Many of the changes in the Auger line shape due to the trends in these processes are not seen so clearly in conventional Auger singles spectra. APECS is able to demonstrate and measure each of these features separately, thereby simplifying complex Auger line shapes. These trends include the following:

(i) A change in the nature of the  $L_3:MM$  two-hole final-state component of the  $L_3-MM$  Auger line from bandlike (Fe, Co) to atomiclike (Ga). Although predominantly atomlike Sawatzky and Haak<sup>1,2</sup> have shown the Cu  $L_{2,3}-MM$  spectrum to have a small bandlike component present at higher kinetic energy that is 7% of the intensity of the atomiclike component. Ni shows both bandlike and atomiclike contributions. The contribution of the two-hole  $L_3:MM$  bandlike component for Ni was found to be  $71 \pm 5\%$  of that of the atomiclike contribution. These changes in the nature of the (two-hole final state)  $L_3:MM$  component contribution to the  $L_3-MM$  Auger spectrum have been seen across the range of the  $3d$  series without the complication of the CK induced  $L_2:L_3:CKMMM$  contribution.

(ii) Quantitative measurement of the change in the rate of the Coster-Kronig transition from being large in Fe, to small in Cu, and not seen at all in Ga. This results in a clearly observed increase in the ratio of the true two-hole final-state  $L_2:MM$  component relative to the three-hole final-state  $L_2:CKMMM$  component of the  $L_{2,3}-MM$  spectra going from Fe to Ga. These measurements make possible a more accurate determination of the energy and transition rate of the CK transitions in the  $L_{2,3}-MM$  Auger lines.

(iii) In the CK decay,  $L_2-L_3M_{4,5}-M_{4,5}M_{4,5}(M_{4,5})$ , the creation of the additional spectator valence-band hole, has the effect of increasing  $U$ , the hole-hole interaction. In the case of Co this results in a narrowing of the  $L_2:L_3:CKMMM$  component of the  $2p_{1/2}$  coincidence spectrum and a shift to lower kinetic energy. The  $L_2:L_3:CKMMM$  component of the  $L_3-MM$  line in Cu is found to be atomiclike, while that of Fe remains bandlike even in the presence of the spectator hole. The best explanation for the Ni results seems to be that the bandlike component of the Ni  $L_2:L_3:CKMMM$  contribution to the  $L_3-MM$  line is absent.

(iv) A detailed accounting for the satellites in the Ga  $L_{2,3}-MM$  Auger line of GaAs. The relative contributions of the intrinsic loss processes is confirmed to be negligible whereas the extrinsic loss function is shown to be a significant consideration when using these lines in quantitative analysis. The second-order plasmons from the  $L_2-MM$  Auger line contribute significantly to the  $L_3-MM$  line and the ratio of surface to bulk-plasmon intensities were shown to vary with changes in inelastic mean free path.

It is clear from the results and discussion that even if the requirement is simply to assay the elemental abundance in a surface then each of the intrinsic and extrinsic processes must be properly accounted for. Both the  $L_2-M_{4,5}M_{4,5}$  and  $L_3-M_{4,5}M_{4,5}$  lines should be used and the area under the low-energy tails of these peaks added for quite some distance below the mainline in order to account for the intensities due to satellites from intrinsic processes. A loss function that

appropriately accounts for the IMFP of the main emission must also be used for background subtraction, particularly for elements such as Ga with significant structure in their extrinsic loss function. Theorists modeling the Auger lines need to know the role of the various intrinsic processes operating in the Auger process and the effect they have on the final line shape. The value of APECS in helping to interpret

the line shapes of complex systems is clearly demonstrated.

#### ACKNOWLEDGMENTS

This work has been well supported by the Australian Research Council (ARC). Two of us (C.P.L. and A.B.W.) have been supported by an ARC funded position.

- <sup>1</sup>H. W. Haak, G. A. Sawatzky, and T. D. Thomas, *Phys. Rev. Lett.* **41**, 1825 (1978).
- <sup>2</sup>G. A. Sawatzky, *Treatise Mater. Sci. Technol.* **30**, 167 (1988).
- <sup>3</sup>D. Coster and R. de L. Kronig, *Physica* **2**, 13 (1935).
- <sup>4</sup>E. Jensen, R. A. Bartynski, and S. L. Hulbert *et al.*, *Rev. Sci. Instrum.* **63**, 3013 (1992).
- <sup>5</sup>S. M. Thurgate, B. Todd, and B. Lohmann *et al.*, *Rev. Sci. Instrum.* **61**, 3733 (1990).
- <sup>6</sup>S. M. Thurgate, *J. Electron Spectrosc. Relat. Phenom.* **81**, 1 (1996).
- <sup>7</sup>C. P. Lund and S. M. Thurgate, *Phys. Rev. B* **50**, 17 166 (1994).
- <sup>8</sup>C. P. Lund, S. M. Thurgate, and A. B. Wedding, *Phys. Rev. B* **49**, 11 352 (1994).
- <sup>9</sup>S. M. Thurgate, *Surf. Interface Anal.* **20**, 627 (1993).
- <sup>10</sup>S. M. Thurgate, C. P. Lund, and A. B. Wedding, *Nucl. Instrum. Methods Phys. Res. Sect. B* **87**, 259 (1994).
- <sup>11</sup>S. M. Thurgate, in *The Structure of Surfaces III*, edited by S. Y. Tong, K. Takayanagi, M. A. Van Hove, and X. D. Xie (Springer-Verlag, Berlin, 1991), Vol. 24, p. 179.
- <sup>12</sup>G. Burns, *Solid State Physics* (Academic, Sydney, 1985).
- <sup>13</sup>C. Kittel, *Introduction to Solid State Physics* (Wiley, New York, 1976).
- <sup>14</sup>D. E. Ramaker, *Crit. Rev. Solid State Mater. Sci.* **17**, 211 (1991).
- <sup>15</sup>J. F. Moulder, W. F. Stickle, and P. E. Sobol *et al.*, *Handbook of X-ray Photoelectron Spectroscopy* (Perkin Elmer Corporation, Eden Prairie, 1992).
- <sup>16</sup>P. Weightman, in *Electronic Properties of Surfaces*, edited by M. Prutton (Adam Hilger Ltd., Bristol, 1984), p. 135.
- <sup>17</sup>H. Aksela and S. Aksela, *J. Phys. B* **7**, 1262 (1974).
- <sup>18</sup>E. D. Roberts, P. Weightman, and C. E. Johnson, *J. Phys. C* **8**, L 301 (1975).
- <sup>19</sup>P. J. Feibelman, E. J. McGuire, and K. C. Pandey, *Phys. Rev. B* **15**, 2202 (1977).
- <sup>20</sup>M. Cini, *Solid State Commun.* **24**, 681 (1977).
- <sup>21</sup>M. Cini, *Phys. Rev. B* **17**, 2788 (1978).
- <sup>22</sup>G. A. Sawatzky, *Phys. Rev. Lett.* **39**, 504 (1977).
- <sup>23</sup>G. A. Sawatzky and A. Lenseink, *Phys. Rev. B* **21**, 1790 (1980).
- <sup>24</sup>W. Bambynek, B. Crasemann, and R. W. Fink *et al.*, *Rev. Mod. Phys.* **44**, 716 (1972).
- <sup>25</sup>E. H. S. Burhop and W. N. Asaad, *Adv. At. Mol. Phys.* **8**, 103 (1972).
- <sup>26</sup>S. B. Whitfield, G. B. Armen, and R. Carr *et al.*, *Phys. Rev. A* **37**, 419 (1988).
- <sup>27</sup>F. J. Himpsel, P. Heimann, and D. E. Eastman, *J. Appl. Phys.* **52**, 1658 (1981).
- <sup>28</sup>J. A. Nedler and R. Mead, *Comput. J.* **7**, 308 (1965).
- <sup>29</sup>S. M. Thurgate and D. E. Erickson, *J. Vac. Sci. Technol. A* **8**, 3669 (1990).
- <sup>30</sup>N. Mårtensson, R. Nyholm, and B. Johansson, *Phys. Rev. B* **30**, 2245 (1984).
- <sup>31</sup>H. W. Haak, Ph.D. thesis, University of Groningen, Groningen, 1983.
- <sup>32</sup>E. J. McGuire, *Phys. Rev. A* **17**, 182 (1978).
- <sup>33</sup>M. Cini, *Solid State Commun.* **53**, 716 (1975).
- <sup>34</sup>M. Cini, *Surf. Sci.* **87**, 483 (1979).
- <sup>35</sup>E. Antonides, E. C. Janse, and G. A. Sawatzky, *Phys. Rev. B* **15**, 1669 (1977).
- <sup>36</sup>E. Antonides, E. C. Janse, and G. A. Sawatzky, *Phys. Rev. B* **15**, 4596 (1977).
- <sup>37</sup>J. van Laar, A. Huijser, and T. L. van Rooy, *J. Vac. Sci. Technol.* **14**, 894 (1977).
- <sup>38</sup>S. Nannone, C. Astaldi, and L. Sorba *et al.*, *J. Vac. Sci. Technol. A* **5**, 619 (1987).
- <sup>39</sup>R. Ludeke and A. Koma, *J. Vac. Sci. Technol.* **13**, 241 (1976).
- <sup>40</sup>N. J. Shevchik, J. Tejada, and M. Cardona, *Phys. Rev. B* **9**, 2627 (1974).
- <sup>41</sup>S. Tanuma, C. J. Powell, and D. R. Penn, *Surf. Interface Anal.* **17**, 911 (1991).
- <sup>42</sup>E. Jensen, R. A. Bartynski, and R. F. Garrett *et al.*, *Phys. Rev. B* **45**, 13 636 (1992).
- <sup>43</sup>F. Yubero, S. Tougaard, and E. Elizalde *et al.*, *Surf. Interface Anal.* **20**, 719 (1993).
- <sup>44</sup>W. Melhorn, *Z. Phys.* **208**, 1 (1968).
- <sup>45</sup>W. Melhorn, B. Bureckmann, and D. Hausmann, *Phys. Scr.* **16**, 177 (1977).
- <sup>46</sup>J. Vayrynen and S. Aksela, *J. Electron Spectrosc.* **23**, 119 (1977).
- <sup>47</sup>M. H. Chen, B. Crasemann, and K. N. Huang *et al.*, *At. Nucl. Data Tables* **19**, 97 (1977).
- <sup>48</sup>S. M. Thurgate, C. P. Lund, and A. B. Wedding, *Phys. Rev. B* **50**, 4810 (1994).
- <sup>49</sup>L. I. Yin, I. Adler, and M. H. Chen *et al.*, *Phys. Rev. A* **7**, 897 (1973).
- <sup>50</sup>J. A. D. Matthew, J. D. Nuttall, and T. E. Gallon, *J. Phys. C* **9**, 883 (1976).